



AC impedance spectroscopy as a technique for investigating corrosion of iron in hot flowing Bayer liquors

Q. LU¹, M.M. STACK² and C.R. WISEMAN³

¹Corrosion and Protection Centre, UMIST, PO Box 88, Manchester, M60 1QD, Great Britain

²Department of Mechanical Engineering, University of Strathclyde, James Weir Building, 75 Montrose St., Glasgow, G1 1XJ, Great Britain

³Banbury Laboratory, Alcan International Ltd, Southam Road, Banbury, Oxon, OX16 7SP, Great Britain

Received 22 November 2000; accepted in revised form 25 July 2001

Key words: Bayer liquors, corrosion, impedance spectroscopy, ion

Abstract

The flow-induced corrosion of iron, in spent Bayer liquor at high temperatures, was investigated using a rotating cylinder electrode (RCE) in an autoclave facility. A temperature range of 100–230 °C and equivalent pipe velocities in the range 0.84–3 m s⁻¹ were used. AC impedance technique was applied to monitor *in situ* the entire corrosion process. Corrosion rates measured by a.c. impedance expressed as average $1/R_p$ were in good agreement with those obtained by weight loss measurements. The results suggest that a.c. impedance is a suitable method to monitor the corrosion process of steels exposed to flowing Bayer liquor at higher temperatures.

1. Introduction

AC impedance technique has been widely used as a corrosion measurement tool. A number of publications have reviewed both the theory and many areas of application [1–5]. These reviews suggest that a.c. impedance is a useful technique for determining mechanistic and kinetic information about the corrosion processes occurring at corroding interfaces.

First, the experimental impedance data $Z(j\omega)_{\text{exp}}$ may be well approximated by the impedance $Z(j\omega)_{\text{equiv}}$ of an equivalent circuit made up of ideal resistors, capacitors, inductors and various distributed elements. In such a circuit, elements represent the various processes involved in the transport of charge and mass in the system being investigated. Various equivalent circuits have been proposed [1, 6, 7] to explain the impedance response of film-covered surfaces, which involve cathodic and anodic reactions in the system.

Second, the use of electrochemical impedance for corrosion rate estimation is well established. In its simple form, the method requires two steps. The frequency response of the corroding electrode is used to obtain the polarization or charge transfer resistance. The current against voltage curve obtained by d.c. polarization is then used to estimate the Tafel slopes. Finally, the corrosion rate (i_{corr}) can be obtained through the Stern–Geary relationship:

$$i_{\text{corr}} = \frac{B}{R_p} \quad \text{or} \quad i_{\text{corr}} = \frac{B}{R_{\text{ct}}} \quad (1)$$

where B is a constant, R_p is the polarization resistance and R_{ct} is the charge transfer resistance. This technique was used for *in situ* corrosion monitoring in the study of corrosion behaviour of steels exposed to spent Bayer liquor at high temperatures.

2. Experimental details

2.1. Rotating cylinder electrode (RCE) test rig

The Bayer process environment was simulated by use of a rotating cylinder electrode system (RCE). This was operated inside a pressurised autoclave to allow high temperatures to be achieved. The corrosion cell consisted primarily of a three-electrode system. Iron was used as a working electrode in each test. Platinum and Hg/HgO (1 M NaOH) electrodes were used as counter and reference electrodes, respectively. The reference electrode was placed inside a separate cell and connected to the test cell through a bridge containing the same Bayer liquor, Figure 1.

After completing assembly of the RCE rig, the fresh deaerated liquor was transferred to the autoclave vessel and reference electrode pot through a closed system. Liquor volumes were 2.5 L and 1 L, respectively. The RCE deaeration facility allowed the liquor to be added whilst still being purged with argon to prevent any ingress of oxygen from the atmosphere. The stirrer was then switched on and a constant flow rate maintained prior to heating the system. Temperature control was

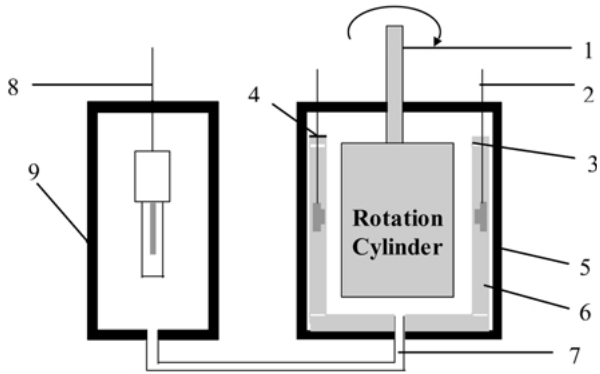


Fig. 1. Schematic of the rotating cylinder electrode and reference cells. Key: (1) rotation cylinder, (2) working electrode, (3) Glyon gasket, (4) counter electrode, (5) autoclave unit, (6) outer cylinder, (7) connection bridge containing same liquor tested, (8) reference electrode, and (9) reference pot.

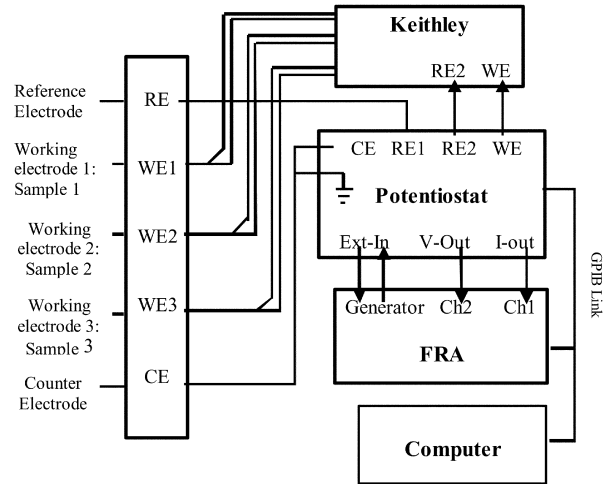


Fig. 2. Schematic of the a.c. impedance measurement facility.

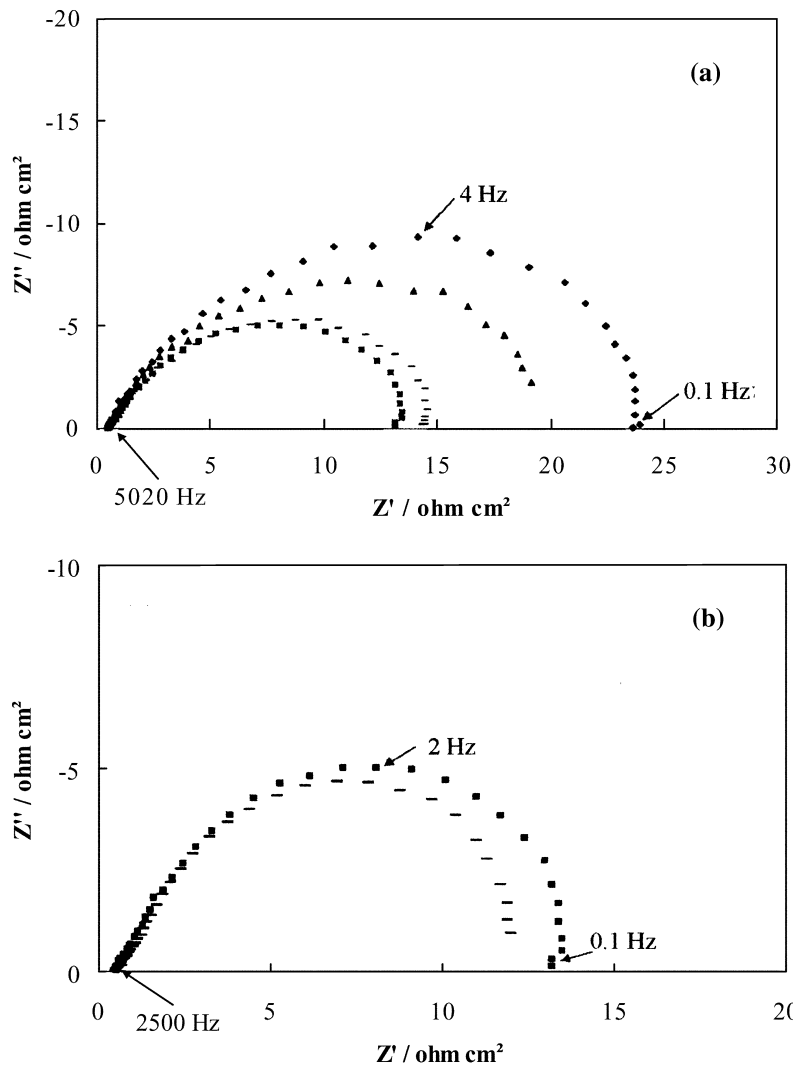


Fig. 3. Measured impedance spectra represented as Nyquist plots for iron exposed to spent Bayer liquor at 1.5 m s^{-1} and $150 \text{ }^\circ\text{C}$. Nyquist plot during (a) first 12 h and (b) final 12 h. Key: (a) \blacklozenge 1, \blacktriangle 3, $-$ 6 and \blacksquare 12 h; (b) \blacksquare 12 and $-$ 24 h.

achieved through the use of two K type thermocouples, one located in the liquor and the other close to the heater band. During heat up polarization at -1.1 V

(vs Hg/HgO 1 M NaOH) was applied to the samples to remove any surface oxide film and also to prevent any further oxide formation during this stage of the test.

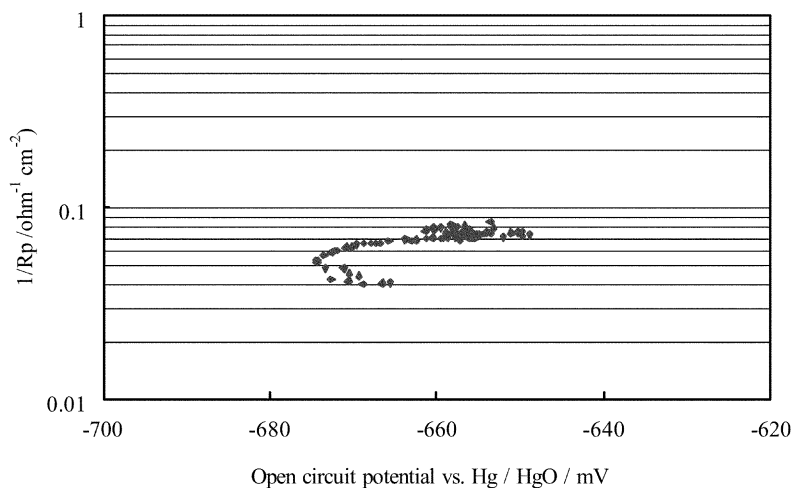


Fig. 4. Polarization resistance of Fe displayed as functions of potential in spent Bayer liquor at 150 °C and 1.5 m s⁻¹.

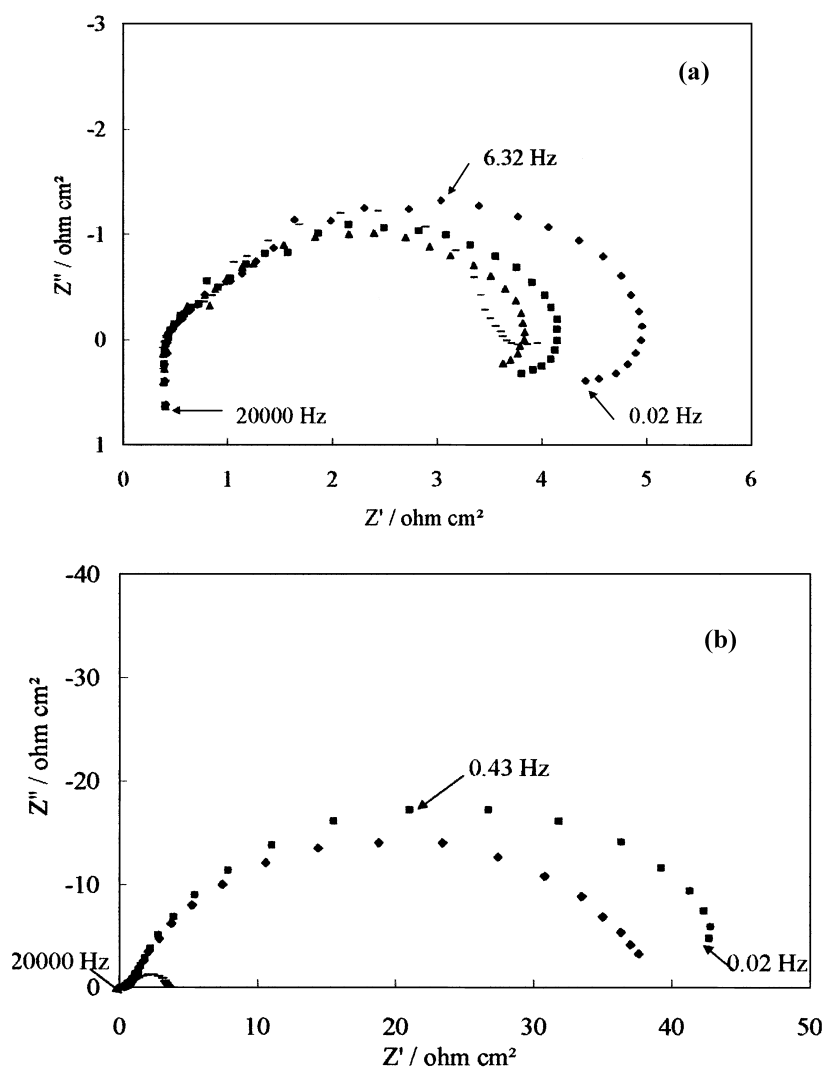


Fig. 5. Measured impedance spectra represented as Nyquist plots for iron exposed to spent Bayer liquor at 230 °C and 0.84 m s⁻¹. Nyquist plot during (a) first 12 h and (b) final 12 h. Key: (a) \blacklozenge 1, \blacksquare 3, \blacktriangle 6 and \blacktriangleleft 12 h; (b) \blacktriangleleft 12, \blacklozenge 16 and \blacksquare 24 h.

AC impedance measurements were started as soon as working temperature was achieved and polarization had stopped. Applied sinusoidal signal ampli-

tude was 10 mV in the nominal frequency range from 10 kHz to 0.02 Hz. A combined frequency response analyser (FRA) and potentiostat (Solartron 1280) was

used to make a.c. impedance measurements under open circuit potential during the test, Figure 2. During each impedance measurement the data were displayed as Bode plots ($|Z|$ and phase angle against frequency) and Nyquist plots (Z_{im} vs Z_{real}) via Z_{plot} software. The data were stored in computer files for analysis after testing.

2.2. Sample preparation

Pure iron (99.9% Fe) was used. The specimens were first polished to a 600 grade silicon carbide paper finish, then rinsed in acetone and deionized water. To simulate surface conditions in the plant, acid cleaning was then carried out at room temperature using a 10% H_2SO_4 solution without inhibitor for 10 min. In the Bayer plant, internal acid cleaning of the pipework etc. is performed regularly to remove surface scale and corrosion products, which can adversely affect the desired heat transfer efficiency and throughput of the plant. The use of this procedure also increased the reproducibility of the specimen-starting surface.

2.3. Test solution

The test solution used in these experiments was spent Bayer liquor; this being plant liquor that has completed

a production cycle. Bayer liquor is essentially pure caustic soda that has been contaminated by impurities from the bauxite ore during the production process. The solution was deaerated, by passing purified argon through it overnight before each test, to reduce any effects due to dissolved oxygen.

2.4. Test conditions

The temperature range varied from 100 to 230 °C with a range of cylinder rotation speeds. Equivalent pipe velocities in the range $0.84-3\text{ m s}^{-1}$ were calculated with reference to the Bayer liquor viscosity, test temperature and rotation speed used [8]. The exposure time was 24 h at the test temperature for each experiment.

3. Results and discussion

3.1. Measured a.c. impedance spectra

Figure 3 shows the results obtained at 1.5 m s^{-1} and 150 °C . The experimental spectra decreased with expo-

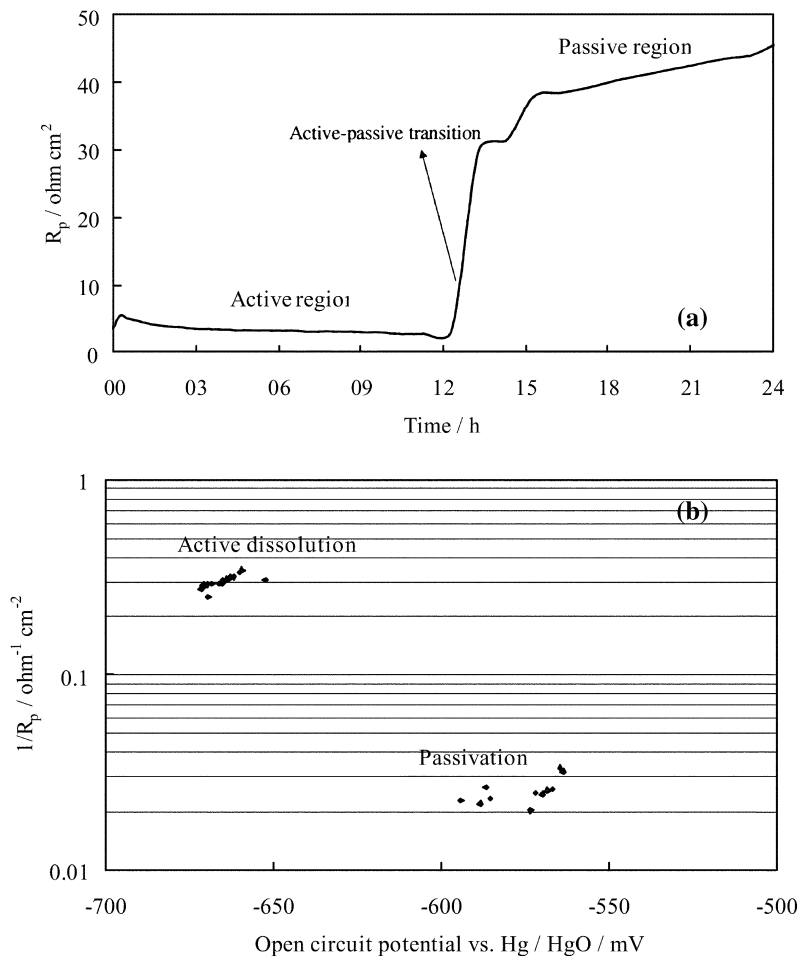


Fig. 6. Polarization resistance displayed as functions of time and potential for Fe exposed to spent Bayer liquor at 230 °C and 0.84 m s^{-1} . (a) R_p against time; (b) $\log 1/R_p$ against potential.

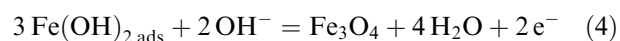
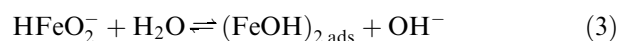
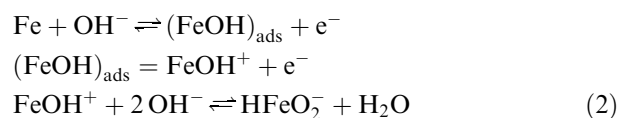
sure time within 6 h of testing, Figure 3(a). After 6 h, any changes in spectra diameter was small, $R_p \approx 15 \Omega \text{ cm}^2$, Figure 3(a) and (b). The open circuit potential was measured and revealed that the potential remained at $-680 \text{ mV vs Hg/HgO}$ during the entire period of the experiment. $\log 1/R_p$ vs open circuit potential was plotted and is presented in Figure 4 for Fe at 150°C . The result indicates that the corrosion process was in a stage of active dissolution at 150°C .

When the temperature was increased to 230°C , an additional inductive loop was observed in the low frequency range. The a.c. impedance spectra for iron at 230°C and 0.84 m s^{-1} are shown in Figure 5. When the exposure time is less than 12 h, two capacitive loops at high and intermediate frequencies and one inductive loop at low frequencies are observed, Figure 5(a). However, after 12 h, the inductive loop disappears and only two semicircles can be seen, Figure 5(b), which coincides with a sudden increase in potential shifted from a constant value of -660 to $-550 \text{ mV vs Hg/HgO}$. After 12 h, the impedance spectra changed slightly and the potential remained at $-550 \text{ mV vs Hg/HgO}$ for the rest of the test period. The results can also be displayed by plotting R_p against time and $1/R_p$ against open circuit potential, Figure 6.

These observations imply that the passive film formation took place retarding the corrosion process by its presence on the metal surface. The results indicated that temperature has a significant effect on a.c. impedance

behaviour. At higher temperatures ($\geq 200^\circ \text{C}$) self-passivation of iron in pure NaOH takes place [9, 10]. The formation of Fe_3O_4 is made easier, due to the fact that higher temperatures drive the reactions (Equations 2–4) in steps in the forward direction. This is in good agreement with the observations found in the current work which shows passivation occurring more readily at 230°C than at 150°C in spent Bayer liquor. Comparing the result in Figure 4 and that in Figure 6(b), they suggest that the corrosion processes were at different stages for iron at 150°C (dissolution) and 230°C (film formation). Alternatively, one of these mechanisms was more dominant depending on the temperature used.

This reaction proceeds in stages [11]:



Topographic and cross sectional SEM examination revealed that very thin surface films were formed at 150°C , Figure 7. Thicker films, which had a crystalline appearance, were seen for this material when tested at 230°C in Figure 8. Evidence of higher corrosion rates in

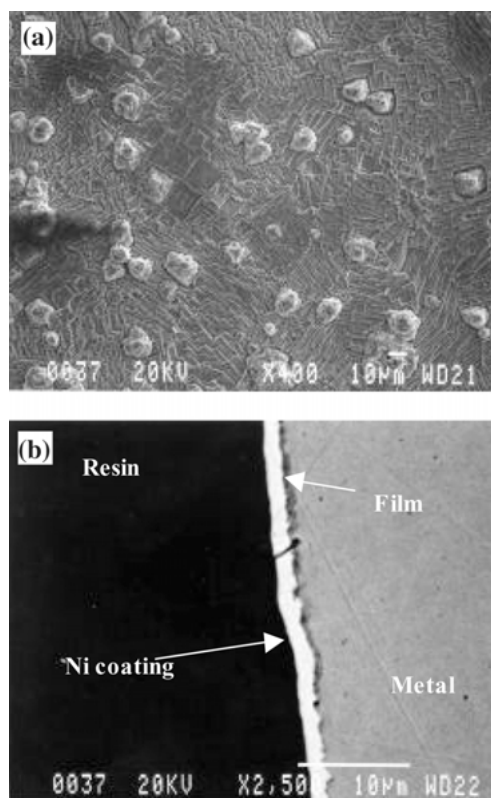


Fig. 7. Fe sample exposed to spent Bayer liquor at 150°C for 24 h at 0.84 m s^{-1} : (a) the surface film at different areas and (b) the cross-sectional view of the surface film.

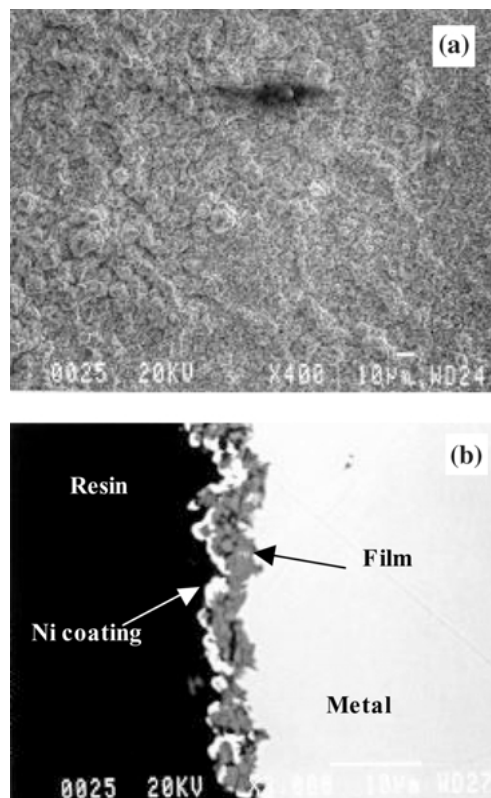


Fig. 8. Fe sample exposed to spent Bayer liquor at 230°C for 24 h at 3 m s^{-1} : (a) the surface film at different areas and (b) the cross-sectional view of the surface film.

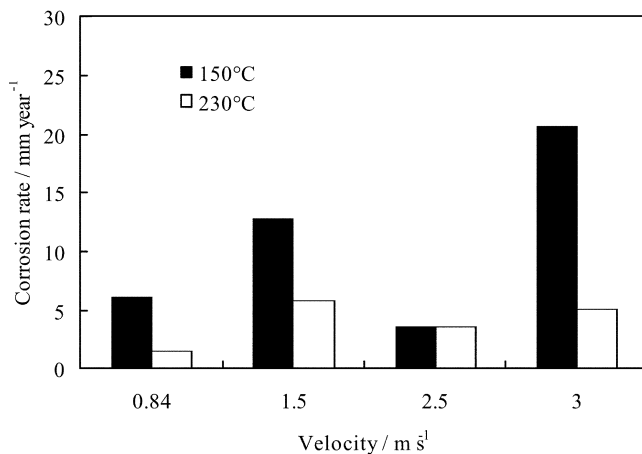


Fig. 9. Effect of liquor velocity on corrosion rate at a range of temperatures for iron.

the range of velocities tested at 150 °C is shown in Figure 9. The results suggest that the corrosion process was being controlled by dissolution at 150 °C, reinforcing the significant velocity effect on corrosion rate. However, at 230 °C, the easier formation of Fe_3O_4 or $\text{Fe}_{3-x}\text{Al}_x\text{O}_4$ [12], which is more stable at high temperatures [13], may have retarded the dissolution process and a lower corrosion rate was observed.

3.2. Comparison of corrosion rates measured by weight loss and $1/R_p$

A comparison of corrosion rate as measured by weight loss and $1/R_p$ is shown in Figure 10. Similar trends in corrosion rate as a function of velocity were shown by both methods.

By applying a correct conversion factor, a corrosion current density, i_{corr} (e.g., in A m^{-2}), can be converted to a penetration rate v_{corr} (mm year^{-1}) as follows:

$$v_{\text{corr}} = \left(\frac{H}{Fd}\right) i_{\text{corr}} = \left(\frac{H}{Fd}\right) \frac{B}{R_p} \quad (5)$$

where v_{corr} is the corrosion rate expressed in mm year^{-1} which can be obtained by weight loss; H is the equivalent weight of the metal, defined as the atomic weight divided by the valence; F is the faradaic constant;

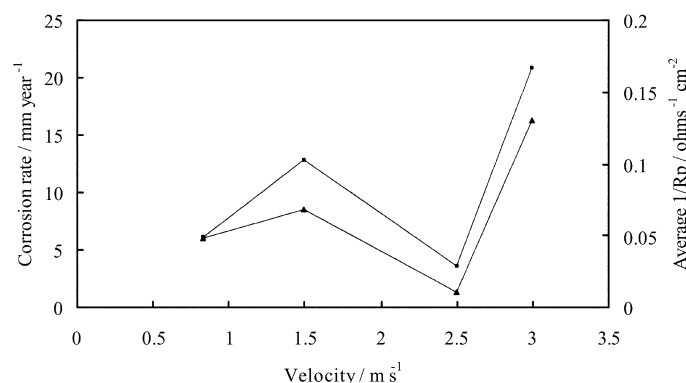


Fig. 10. A comparison of corrosion rate measured by weight loss (●) and $1/R_p$ (▲) at 150 °C for iron exposed to spent Bayer liquor.

Table 1. B values calculated from R_p and weight loss data at 150 °C for iron

Velocity / m s^{-1}	Corrosion rate / mm year^{-1}	Average $1/R_p$ / $\Omega^{-1} \text{cm}^{-2}$	B / mV
0.84	6.1	0.05	14.4
1.5	12.8	0.07	21.4
2.5	3.6	0.01	38.9
3	20.7	0.13	18.2
Average B value			23.2

d is the density of the metal; and B is a constant. An average B value of 23 mV (Table 1) was determined from R_p and weight loss data according to (Equation 5). This is close to the value of 25 mV reported for corrosion of steels in aqueous environments [14] and also near to the empirical value of 30 mV determined through the use of plant probes in Bayer liquor environments.

4. Conclusions

- AC impedance is identified as a suitable method to monitor the entire corrosion process of steels exposed to flowing Bayer liquor at higher temperatures.
- Corrosion rates measured by the electrochemical method ($1/R_p$) showed similar trends to those measured by the weight loss. The B value of iron, in spent Bayer liquor, was obtained using weight loss and R_p data. The value of 23 mV is similar in magnitude to values calculated by other workers.
- The results indicate that temperature has a significant effect on a.c. impedance behaviour. At 150 °C the corrosion process was dominated by active dissolution and less film was formed on the metal surface. This mechanism enhances the effect of velocity on both the corrosion rate and surface film morphology. The results imply that in the absence of, or with only small amounts of surface film present at the surface, velocity has a significant effect on the corrosion rate of iron. The results also suggest that increasing the temperature enables

passivation to take place more readily, thus reducing the corrosion rate.

Acknowledgements

This project was financially supported by Alcan International Limited, Banbury. The authors appreciate the contribution of Drs R.C. Furneaux, J. Sharman and C.J. Newton. Also thanks are given to J. Bradley and A. Spencer for carrying out many of the RCE tests.

References

1. S. Turgoose and R.A. Cottis, The impedance response of film-covered metals, Conference Proceedings: 'Electrochemical Impedance Analysis and Interpretation', San Diego, CA (1991) (ASTM STP 1188).
2. P. Li, T.C. Tan and J.Y. Lee, *Corros. Sci.* **38** (1996) 1935.
3. D.C. Silverman and J.E. Carrico, *Corrosion* **44** (1988) 280.
4. D.D. Macdonald and M.C.H. McKubre, 'Electrochemical Impedance Techniques in Corrosion Science', *Electrochemical Corrosion Testing*, ASTM STP 727 (1981) 110.
5. F. Mansfeld, *Corrosion* **44** (1988) 856.
6. A. Bonnel, F. Dabosi, C. Delouis, M. Duprat, M. Keddad and B. Tribollet, *J. Electrochem. Soc.* **130** (1983) 753.
7. K. Juttner, W.J. Lorentz, M.W. Kending and F.J. Mansfeld, *J. Electrochem. Soc.* **135** (1988) 332.
8. N.A. Darby, C.J. Newton and J.D.B. Sharman, 'Simulations of Bayer liquor pipeflows using a rotating cylinder electrode', submitted to TMS Light Metals (1999).
9. G.J. Bignold, *Corros. Sci.* **12** (1972) 145.
10. R.L. Jones, L.W. Strattan and E.D. Osgood, *Corrosion* **26** (1970) 399.
11. D. Geana, A.A. El Miligy and W.J. Lorenz, *J. Appl. Electrochem.* **4** (1974) 337.
12. R. Sriram and D. Tromans, *Corros. Sci.* **25** (1985) 79.
13. B.D. Craig, 'Fundamental Aspects of Corrosion Films in Corrosion Science' (New York, 1991), p. 17.
14. F. Mansfeld, The polarization resistance technique for measuring corrosion currents in M.G. Fontana and R.W. Stachle (Eds), 'Advances in Corrosion Science and Technology', Vol. 6, (Plenum Press, New York, 1976).